

**FLEXURAL STRENGTH CAPACITY FOR
HOBBS BUILDING SYSTEMS'
"HOBBS VERTICAL ICF WALL SYSTEM"**

BY: DR. MAX L. PORTER, BRANDON O. VILAND

JANUARY 15, 2009

FINAL PROJECT REPORT

**CIVIL, CONSTRUCTION AND ENVIRONMENTAL
ENGINEERING DEPARTMENT**

**IOWA STATE UNIVERSITY
AMES, IOWA**

Disclaimer

The contents of this report do not represent a warranty of the products used on behalf of Iowa State University, or the authors of the report. The Engineering data and conclusions presented have been determined in accordance with professional principles and practices. In addition, the data and conclusions are for general information purposes only and should not be used without competent advice with the respect to their suitability for any given application. Therefore, the responsibility for the use of the information in the presented report remains with the user. The report is intended for information purposes only and is made available with the understanding that it will not be altered without the permission of the authors.

TABLE OF CONTENTS

Abstract.....	vi
Introduction.....	- 1 -
Literature Review	- 2 -
Experimental Phase	- 5 -
Full-Scale Wall Tests.....	- 5 -
Specimen Characteristics	- 5 -
Material Properties	- 13 -
Full-Scale Test Procedure.....	- 19 -
Behavioral Results.....	- 25 -
Analysis of Results.....	- 29 -
Full-Scale Wall Test	- 29 -
Summary and Conclusions	- 39 -
Acknowledgements	- 41 -
References:.....	- 42 -

LIST OF FIGURES

Figure 1. “HOBBS Wall” Composite Section	6 -
Figure 2. Beam Cross-Section at the Web (Top Beam left, Bottom Beam right)	7 -
Figure 3. Side View of EPS foam formwork.....	8 -
Figure 4. Top View of the EPS foam formwork.....	8 -
Figure 5. Furring Assembly and Retainer Clip	9 -
Figure 6. View of the Top Beam Formwork with Steel Reinforcement in Place	10 -
Figure 7. Constructed Wall Specimens	11 -
Figure 8. Concrete Slump	12 -
Figure 9. Steel Reinforcement Tensile Test Results	17 -
Figure 10. Magnified Plot of Steel Yielding.....	18 -
Figure 11. Theoretical 4-Point Loading Scheme	19 -
Figure 12. Full-Scale Test Set-Up.....	21 -
Figure 13. Loading Ram and Load Cell	22 -
Figure 14. Displacement Transducer Placement.....	23 -
Figure 15. Displacement Transducer Attached to the Specimen.....	23 -
Figure 16. Fabricated Abutment on Pinned-End	24 -
Figure 17. “HOBBS Wall” Force-Displacement	26 -
Figure 18. Flexural-Shear Cracking of the Specimen	27 -
Figure 19. Compression Buckling on the Top Flange of the Furring Assembly.....	28 -
Figure 20. Furring Assembly Failure, "Necking" (left) and Fracture (right)	28 -
Figure 21. Idealized Force-Displacement Comparison	38 -

LIST OF TABLES

Table 1. Concrete Mix Data.....	- 13 -
Table 2. Concrete Cylinder Strength Test Results.....	- 14 -
Table 3. Modulus of Rupture Test Results	- 15 -

LIST OF CALCULATIONS

Calculation 1. Determining Loading Location	- 20 -
Calculation 2. Determining Moment Induced by the Self Weight.....	- 30 -
Calculation 3. Equivalent Distributed Load	- 31 -
Calculation 4. Theoretical Cracking Moment.....	- 32 -
Calculation 5. Theoretical Cracking Load.....	- 33 -
Calculation 6. Theoretical Nominal Moment Strength	- 34 -
Calculation 7. Load Corresponding to Nominal Moment	- 35 -
Calculation 8. Theoretical Displacement.....	- 36 -

ABSTRACT

The purpose of this research and testing was to determine the flexural strength capacity of the HOBBS Building Systems' "HOBBS Wall" insulated concrete form wall system. The scope of the project included flexural testing and analysis of two full-scale wall specimens. The wall specimens were 10 ft 4 in. tall and 4 ft wide, subjected to a simply supported four-point loading scheme.

The results of the flexural testing determined that the flexural capacity of the "HOBBS Wall" system benefits substantially from composite action; reaching an average flexural strength capacity of 14.56 k-ft for the 4 ft wide full-scale wall specimens tested, an increase of approximately 4.80 k-ft over that of a comparable reinforced concrete section that was analyzed.

INTRODUCTION

Insulated Concrete Form (ICF) construction is composed of layers, or wythes, of concrete and rigid foam. The particular ICF design that is investigated in this study has concrete cast between a rigid foam exterior. The foam stays in place and serves as a very effective insulation and sound barrier. With the price to heat a home as it is today, there has been an increased urgency to use energy efficient building methods in both the residential as well as the commercial spectrum. ICF construction is a desirable alternative to standard masonry wall construction since the ICF wall contains insulation and water proofing within the system itself. ICF walls also do not require interior framing on which to attach the drywall or interior finish since there are dense plastic strips embedded vertically every 16 inches. All these properties that are inbuilt with the ICF wall system reduce the number of trades required on the job; and therefore, reduce the expense of manual labor as well as effectively expedite the progress of the project.

The conventional Insulating Concrete Form wall system has typically been of uniform thickness throughout. The “HOBBS Wall” system uses a concept of beams and columns with much thinner webs between. The idea is that the lateral soil pressure will be sufficiently supported by the steel-reinforced columns and the vertical building loads by a combination of the beams and columns; therefore, the largely decreased amount of concrete in the webs should not jeopardize the structural integrity of the system.

The HOBBS Building Systems company was interested in investigating the flexural strength capacity of their “HOBBS Wall” design. This report covers the testing of two full-scale “HOBBS Walls”, 124 inches tall by 48 inches wide, for flexural

capacity. Upon completion of testing, the data was analyzed and then compared to conventional steel-reinforced concrete wall systems.

LITERATURE REVIEW

Insulating Concrete Form (ICF) construction has been around for quite some time; it was invented in the 1940's in Europe and really evolved with the advancement of modern plastic foams and molding technologies during the 1960's. It wasn't until the 1980's that ICF construction became more widely used in North America; although there were not many companies that practiced this construction procedure. By the mid-1990's ICF construction increased substantially in the United States as contractors became more adept with the method. Following this, ICF construction has continued to grow at a significant rate in the U.S. (1)

There are a multitude of advantages in using an Insulated Concrete Form system versus conventional building techniques. The start-up cost of an ICF system is still slightly higher than that of a framed building, but over-time this initial cost is more than made up for in energy savings. ICF construction has insulation and framing built into it, therefore, reducing the number of trades on the job and thus reducing the project expense. The main advantages of ICF come in the form of energy efficiency. The high insulation rating of the system is reported to account for approximately 25 to 50 percent decrease in Heating, Ventilating, and Air Conditioning (HVAC) energy consumption between an ICF house to that of a comparable frame house, although the thermal insulating properties of the "HOBBS Wall" system was beyond the scope of this project.

The term thermal mass relates to the ability of a body of mass to absorb and store heat without significant increases in that body's temperature; therefore, greatly reducing

the heat flow through the medium and out the other side. A substantial concrete wall has several times the thermal mass than that of a comparable frame wall; therefore, the much more massive concrete wall stays at a more consistent temperature. In some cases the property insurance provider may offer reductions in home owner's insurance for houses built with high fire and wind resistance, termed "superior construction". (2)

Iowa State University has done research on different aspects of Insulated Concrete Form walls in the past. One such study, *Elemental Beam and Shear Testing of GFRP Sandwich Wall Connectors*, dealt with investigating slab flexure capacity. From this, interest was given to the amount of benefit that was discovered to be contributed by the composite action of the Expanded Polystyrene (EPS) foam. There is not a direct relation although, since the walls tested in the study were comprised of two concrete wythes making up the exterior with a layer of foam between. But nevertheless the paper provided useful information into the current understanding of sandwich wall behavior. The report determined a percentage that was to be representative of the contribution to the nominal moment capacity of the section acting as fully composite versus not composite. The tests were conducted with varying amounts and types of connectors between the concrete wythes. Average percentages of contribution ranged from 29% to 43% for fiber reinforced plastic (FRP) truss connectors and 23% to 43% E-glass fiber/polyester resin connectors. Therefore, there was determined a fairly significant increase in the flexural capacity of the walls tested. Now whether this phenomenon of flexural strength increase can be related to the "HOBBS Wall" system, offers some debate; but it is apparent that the composite action is beneficial to the flexural strength. (3)

Walls such as this, with the concrete wythes on the exterior, are more likely to see large temperature differentials through the depth since the concrete, an effective medium of heat transfer, is exposed directly to the ambient air temperature. In a study entitled, *Heat Transfer Characteristics of Insulated Concrete Sandwich Panel Walls*; EPS foam was found to have a thermal conductivity of $0.22 \text{ (Btu} \cdot \text{in.)}/(\text{hr} \cdot \text{ft}^2 \cdot ^\circ \text{F})$; while normal weight concrete has a reported thermal conductivity of $16.0 \text{ (Btu} \cdot \text{in.)}/(\text{hr} \cdot \text{ft}^2 \cdot ^\circ \text{F})$ (4) Therefore, one could conclude because of the great difference in thermal conductivities, the two concrete wythes could potentially be temperatures of significant difference due to the layer of foam between preventing heat flow across the thickness. This differential may prove to result in cyclic heating and cooling of the concrete wythes, depending on the climate, which, due to expansion and contraction can break the bond of the concrete to the EPS foam, thus taking away from the benefit due to the composite action of the section. Research has been done here at Iowa State University on concrete sandwich walls subjected to temperature differentials across their thickness. The study entitled, *Thermal and Fatigue Testing of Fiber Reinforced Polymer Tie Connectors Used in Concrete Sandwich Walls*; study the effects of a 100°F temperature differential on three full-scale 40'-0" wall panels. The walls incorporated Delta Tie[®] fiber reinforced polymer tie connectors, connecting the concrete wythes across the center foam wythe and found that the Delta Tie[®] performed well against in-plane shear due to longitudinal thermal bending. (6)

EXPERIMENTAL PHASE

In the following section the experimental phase of the project will be described. The experiments were conducted in Iowa State University's structural laboratory. The testing apparatus for the "HOBBS Wall" tests was fabricated and constructed during the months of June and July of 2008.

Full-Scale Wall Tests

The flexural strength capacity test was conducted to determine the nominal moment capacity of the full-scale wall system. The test provided valuable insight into the validity of the current wall design in resisting imposed moments from lateral loads.

Specimen Characteristics

The HOBBS Building Systems' "HOBBS Wall" is unique in that the formwork greatly reduces the amount of concrete used as compared to comparable ICF building systems with uniform thickness. Different from other systems; the walls are comprised of beams, columns, and webs.

The 'columns' incorporated in the wall system are located 16 inches on center spacing and are cast at the location of the furring assemblies. For the particular wall size tested, the columns are 4 inches wide and 5.25 inches deep in the direction resisting the lateral loads. The vertical steel-reinforcement in the columns is attached directly to the furring assemblies and held in place during casting with small Poly-Vinyl Chloride (PVC) clips. The reinforcement in the columns is a single #5 (5/8 in. diameter) grade 60 steel reinforcing bar; one per column. The reinforcement is clipped into place favoring what will be the tension side of the wall due to the lateral loads; therefore nearer the

interior of the structure. The effective depth of the reinforcing bar in the column is 3.75 in. from the compression face of the column, and is centered with respect to the width of the column. The “HOBBS Wall” system can be seen in Figure 1, showing the composite section of the wall.

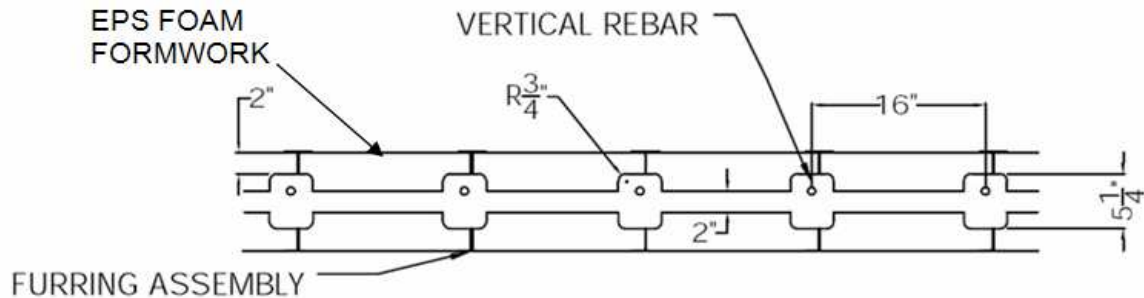


Figure 1. “HOBBS Wall” Composite Section

The ‘beams’ incorporated in the wall system are located at both the top and bottom of the wall; the top beam is 12 inches deep and 5.25 inches wide with a short 45° chamfer to reduce from 5.25 inches to the web thickness of 2 inches. The bottom beam is triangular shaped; 5.25 inches at the base and 7 inches tall, the sides are at an 11° angle to the vertical. There are single horizontal reinforcing bars for both the top and bottom beams. The top beam reinforcing bar is placed in notches located in the furring assemblies, and the bottom beam reinforcing bar is either placed in the notches at the bottom of the furring assemblies or tied to the footing dowels at the appropriate location. The horizontal reinforcement in the top beam is located at the mid-width of the beam, 5.75 inches down from the top. The bottom beam reinforcement is also located at mid-width, 3 inches up from the bottom of the wall. Design sketches of the top and bottom beams can be seen below in Figure 2.



Figure 2. Beam Cross-Section at the Web (Top Beam left, Bottom Beam right)

The ‘webs’ of the wall system are bordered by the beams and columns. They are not steel-reinforced and are 2 inches thick. The incorporation of the webs makes the “HOBBS Wall” more efficient since the concrete thickness is reduced where it is not needed for structural integrity and greatly increases the energy efficiency of the wall by filling the rest of the wall thickness with insulating foam.

The Expanded Polystyrene (EPS) foam acts as the formwork for the concrete core, as well as a very effective insulator. The EPS is 2 inches thick on either side at the beams and columns and 3.625 inches thick on either side at the webs. Design sketches of the EPS foam formwork can be seen in Figure 3 and Figure 4 below. The EPS foam forms achieve an insulation R-Value of approximately 30; making the home or business more energy efficient and saving the owner money on heating and cooling bills. The term ‘R-Value’ is simply a number rating that represents the material’s quality of resisting heat flow. Considering a new residence, natural gas furnace and electric air conditioning, the Department of Energy suggests providing an insulation R-Value of 11 to 12 for basement foundation walls in a climate typical of the Midwest (5).

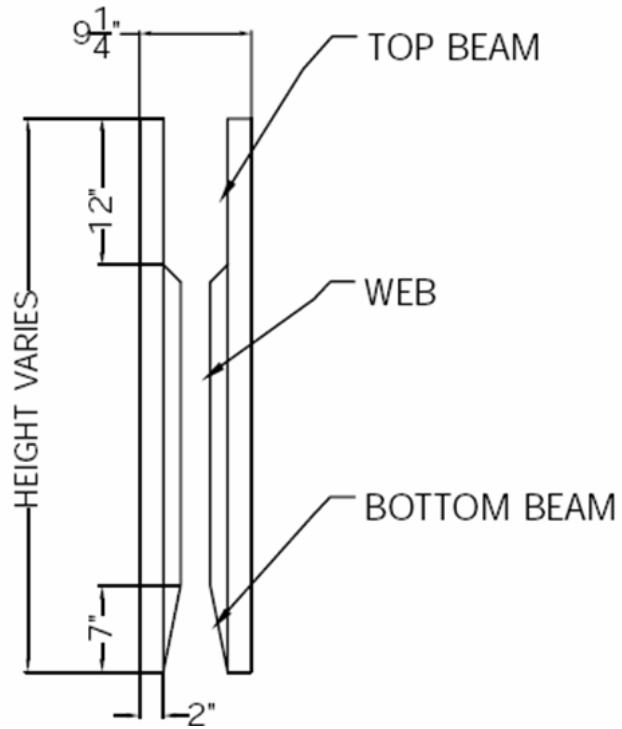


Figure 3. Side View of EPS foam formwork

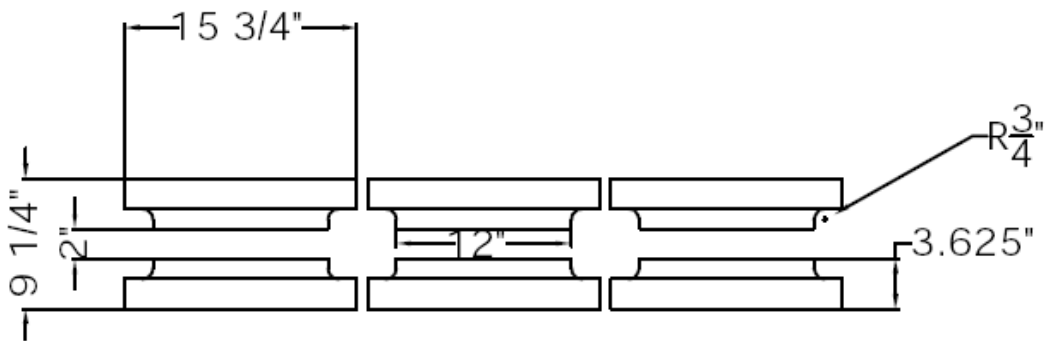


Figure 4. Top View of the EPS foam formwork

The furring assemblies are made of Polyvinyl Chloride (PVC); they are I-shaped, 9.5 inches deep with 2.5 inch flanges. The flanges and web are 0.125 inches thick. Throughout the web are a series of holes and notches in which the steel reinforcing bars may be placed. The notches provide support for placing the horizontal bars, and the holes can be fitted with retainer clips that are used to hold the vertical bars in place as well as hold the foam formwork in position. The notches and retainer clips as was seen in the test specimens are shown in Figure 5 and Figure 6.

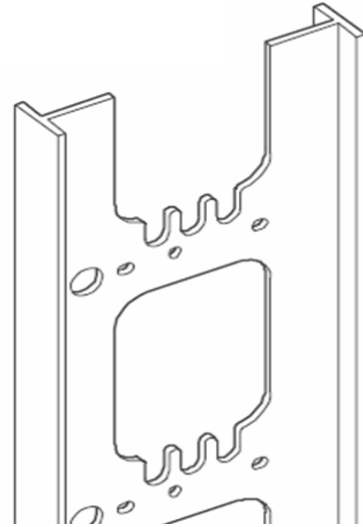


Figure 5. Furring Assembly and Retainer Clip

Both of the wall specimens contained two furring assemblies, located at third points along the width.



Figure 6. View of the Top Beam Formwork with Steel Reinforcement in Place

The wall specimens were constructed and cast on 04-June, 2008 by the HOBBS Building Systems crew with help from students at Iowa State University. There were two wall segments constructed; 4 feet wide and 10 feet 4 inches tall. The walls were constructed to be free-standing using timber braces along with the EPS foam forms and furring assemblies as shown in Figure 7. To start, the crew fastened two PVC angles, parallel to each other and 9.5 inches apart, to a 1 in. x 12 in. by 4 ft long timber board. Two separate furring assemblies were then fastened to two 2 in. x 10 in. planks by 10 ft 4 in. long; these will be on the ends of the wall segments and will help provide formwork and support during the casting process. The 1 in. x 12 in. timber with the angles was laid down and one of the 2 in. x 10 in. planks with the furring assemblies fastened to it was stood up at the end of the 1 in. x 12 in.; two EPS foam panels were slid into position

against the plank followed by another furring assembly and so on with the final furring assembly being attached to the other 2 in. x 10 in. plank. The walls were stood upright using two 2 in. x 4 in. angled braces on each side.



Figure 7. Constructed Wall Specimens

Upon delivery of the concrete a slump test was conducted and a slump of 4.5 in. was measured as can be seen in the illustration of Figure 8. The concrete was poured into the wall forms using an overhead bucket. The first wall was poured in a single lift, and then vibrated with a probe over the top half and vibrated/consolidated externally over the bottom half. The second wall was poured in three approximately equal lifts and vibrated with an electric probe vibrator after each lift.



Figure 8. Concrete Slump

Along with casting the walls, 15 – 6 inch diameter by 12 inch tall concrete cylinders were cast. Typically 12 cylinders is sufficient since it is standard to test 3 cylinders at a time on 7 day increments; ie. 7-day, 14-day, 21-day, and 28-day strength tests. There was extra concrete, and since the experiment was to attempt to target a concrete strength of 3,500 psi, additional cylinders were thought to possibly be necessary. Casting the additional cylinders proved very fortunate because the 28-day strength was not adequate and a longer curing period was required; in fact the total curing time was 57 days. Along with the cylinders, 3 - 6 inch square modulus of rupture beams, capable of two breaks each, were cast in order to get an actual experimental modulus of rupture value. Both the strength cylinders and the modulus beams were cast in three lifts and first uniformly rodded 25 times over the entire area then the mold was tapped 10 to 15 times for each lift as per ASTM – C31.

Material Properties

The specified concrete strength ordered from Iowa State Ready Mix was to be 3,000 psi with a slump of 4 inches; and although the target concrete strength for testing was to be 3,500 psi; 3,000 psi was ordered since the mix is typically of considerably higher strength than what is ordered. The concrete batch was 1.25 cubic yards and the mix composition can be seen in Table 1.

Table 1. Concrete Mix Data

Concrete Mix (per 1.25 yd):	
Cement -	562 lb
3/8" - Cracked Agg. -	2160 lb
Sand -	1960 lb
Water Reducer -	187.33 oz.
Air Entraining	1.875 oz.
Water -	14-15 gal.

The concrete test cylinders were tested in a concrete cylinder compression testing apparatus using neoprene pads on the top and bottom faces of the cylinders per ASTM C39. Upon testing the first three cylinders at seven days, it was rather apparent that there was going to be an issue with the strength of the concrete as the strength of the cylinders only averaged 1996 psi. At 13 days another three cylinders were tested and the average was only 2,172 psi, thus giving a strength increase of approximately 200 psi. The cylinders tested approximately every seven days following showed similar strengths increases as can be seen in Table 2. After the three cylinders were tested for 28-day strength; as is the standard for reaching specified concrete strength, it was deemed that the concrete was not yet of sufficient strength and thus was determined it would be best

to wait longer to allow the concrete to continue to gain strength. Testing was chosen to take place on 31-July, 2008; the final three concrete test cylinders were tested the morning of test day and proved to yield an average strength of 2448 psi.

Table 2. Concrete Cylinder Strength Test Results

Days Elapsed	Date	Cylinder No.	Concrete Strength (psi)	Average (psi)
7	11-June, 2008	1	1887	1995.7
		2	1995	
		3	2105	
13	17-June, 2008	4	2225	2172.3
		5	2145	
		6	2147	
22	26-June, 2008	7	2397	2421.0
		8	2420	
		9	2446	
28	2-July, 2008	10	2349	2372.7
		11	2335	
		12	2434	
57	31-July, 2008	13	2392	2448.0
		14	2495	
		15	2457	

The strength ended up much lower than was preferred although it was deemed acceptable to move forward with the testing, as the lower strength concrete may provide some valuable insight.

From the tested concrete strength one can determine the estimated Modulus of Rupture (f_r) of the concrete using a simple calculation given by Equation 1.

$$f_r = 7.5\sqrt{f'_c} \quad \text{Equation 1}$$

where:

f_r = Modulus of Rupture (psi)
 f'_c = Concrete Strength (psi)

With the concrete strength on test day of 2,448 psi; this equation yields a flexural modulus of rupture of 371.1 psi. The modulus of rupture for the concrete was also determined experimentally using the modulus of rupture beam specimens cast along with the wall specimens and test cylinders. There were three beam specimens allowing two tests per beam. The tests were conducted in accordance with ASTM C78 method, the flexural strength of concrete beam specimens having a cross section of 6 inches by 6 inches and using a span length of 18 inches for testing. A beam testing machine was used (Model S6). A total of six tests were conducted; these yielded an average modulus of rupture of 372.2 psi. A complete tabulation of the results can be seen in the following Table 3.

Table 3. Modulus of Rupture Test Results

Specimen	Trial	Dial Reading			Factored Value	
		Load (lb)	fr (psi)	Factor	Load (lb)	fr (psi)
Beam #1	#1	4200	350	0.99	4158.00	346.50
	#2	4380	365	0.99	4336.20	361.35
Beam #2	#1	4344	362	0.99	4300.56	358.38
	#2	4452	371	1.00	4452.00	371.00
Beam #3	#1	4560	380	0.99	4514.40	376.20
	#2	5040	420	1.00	5040.00	420.00
Average:		4496.00	374.67		4466.86	372.24

The factor value in the table accounts for the cross-section of the modulus beam differing from 6 inch by 6 inch. The trials with a factor of 0.99 had a beam width of slightly more than 6 inches and therefore the modulus of rupture value could not simply be taken as the dial reading. Notice the average experimental value, 372.24 psi, proved to be quite close to that of the calculated value, 371.1 psi.

The test specimens were cast using #5 Grade 60 steel-reinforcement. A #5 bar has a nominal diameter of $\frac{5}{8}$ " and nominal strength of 60,000 psi. As is common practice in the steel industry, grade 60 steel is often capable of much greater strength. Three steel-reinforcement specimens were prepared to be tested for tensile strength. The specimens were 12" long and tested using the SATEC™ testing machine. The three specimens proved to show yield strengths of 63,900 psi, 63,700 psi, and 64,000 psi; giving an average of approximately 63,867 psi. The three specimens reached an ultimate strength of 102,613 psi, 103,023 psi, and 103,119 psi respectively; yielding an average ultimate strength of 102,918 psi. The following plots, Figure 9 and Figure 10, show the test results of the steel reinforcement. Notice in Figure 9 how the yield plateau as well as the ultimate strength reached by the three specimens is nearly identical. Then in the following plot, Figure 10, the slight discrepancies of the yield strengths are more easily seen.

In observing this particular region of the graph more closely, one can see where the slope of the stress-strain plot changes and begins to plane out. The exact yield point of each steel specimen may be debatable, although the location should be where a significant change in slope occurs.

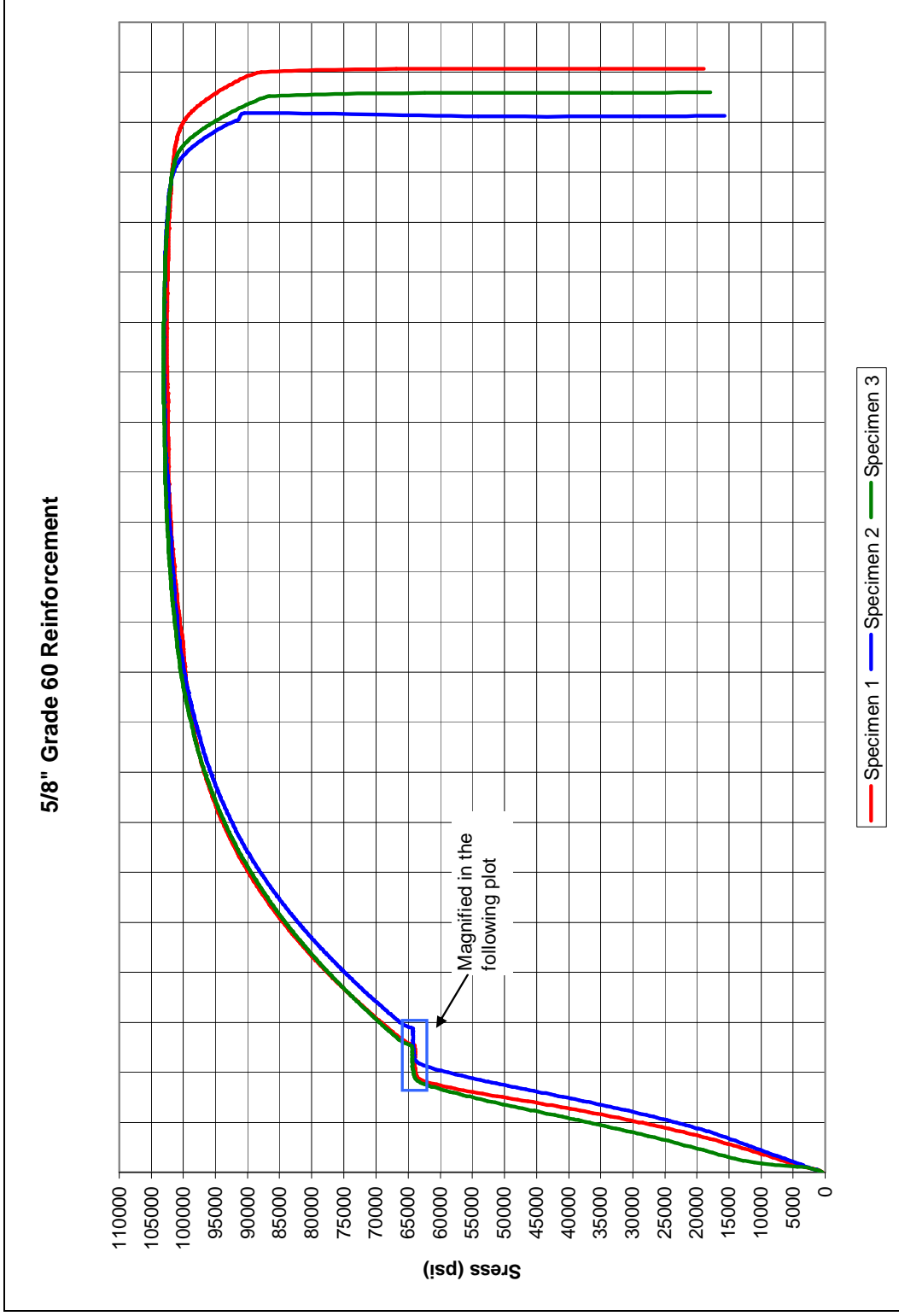


Figure 9. Steel Reinforcement Tensile Test Results

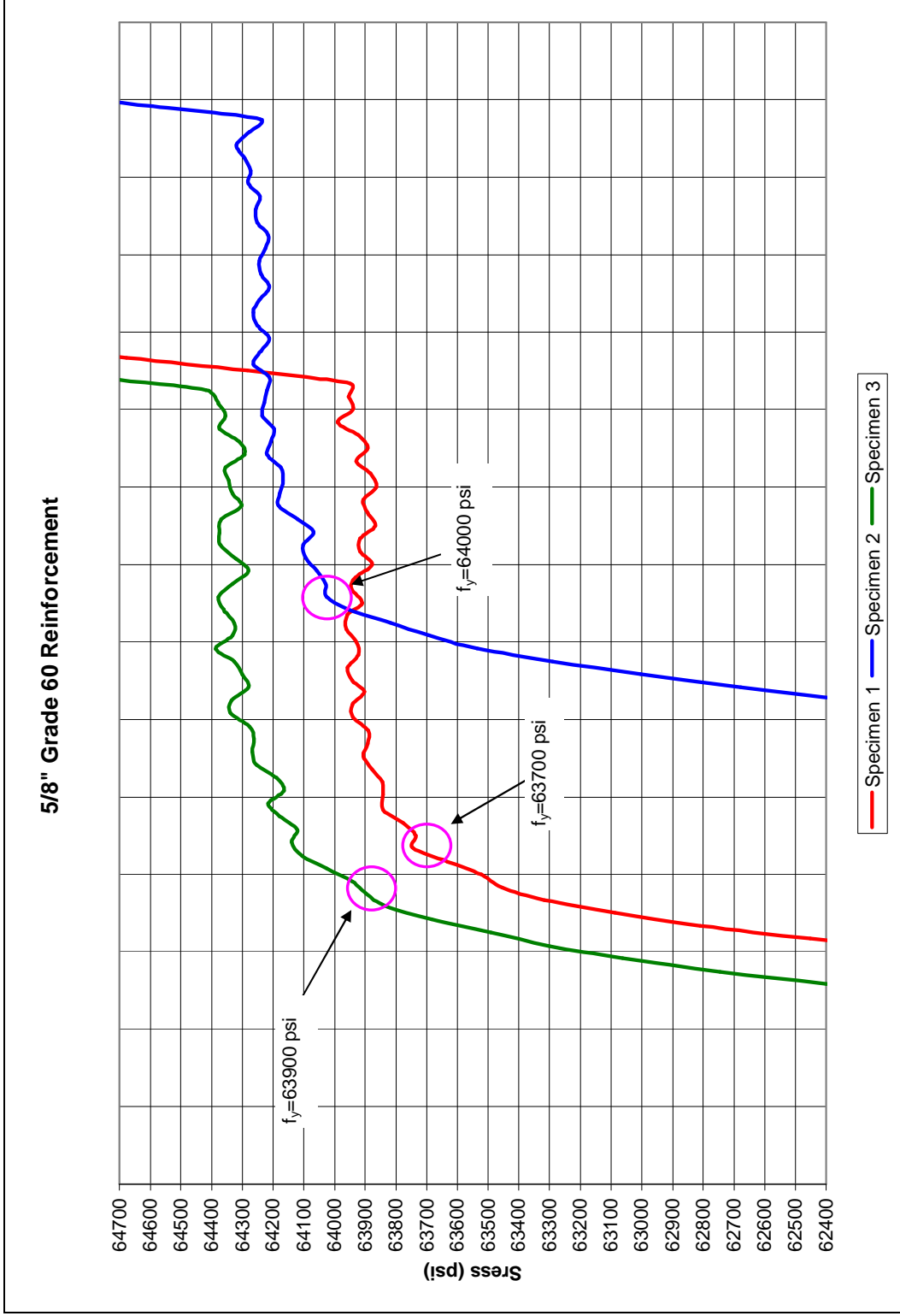


Figure 10. Magnified Plot of Steel Yielding

Full-Scale Test Procedure

The testing was conducted using an equivalent four-point loading scheme that has been found to closely resemble the action of distributed loading. The line loads were positioned ($\ell/4$) distance from the supports, thus providing a space between of ($\ell/2$); where ℓ represents the span length. In theory the test set-up is as seen in Figure 11.

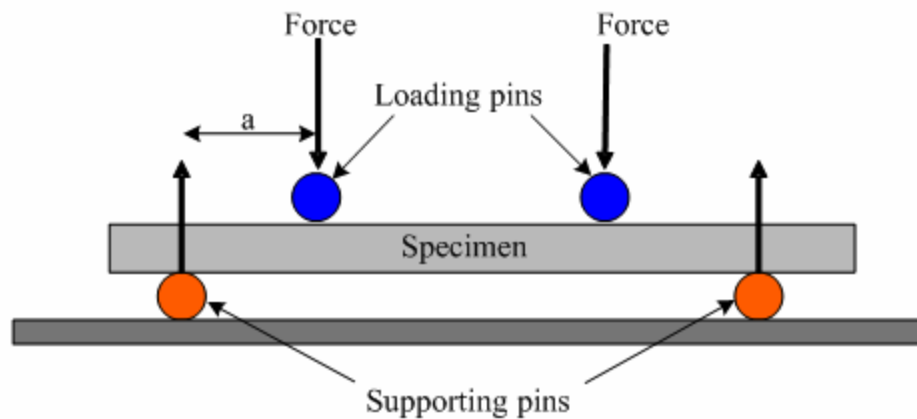


Figure 11. Theoretical 4-Point Loading Scheme

The test frame was a simple H-frame set-up consisting of vertical uprights and a main beam; post-tensioned down to the floor with a force of 12,000 lbs on each side. The main beam was a 12 inch by 6 inch rectangular tube. The loading device, a 10-ton hydraulic loading ram, was secured in place to the main beam and centered on the specimen. Since the loading ram is only going to see significant forces in compression, the ram was simply held up in place by large C-clamps. Under the ram, running lengthways to the wall specimen, were two beams, W6x9. These beams transferred the load from the loading ram to two 6-inch square steel tubes located at $\ell/4$ (29.5 inches) from the end supports.

Calculation 1. Determining Loading Location

$$\frac{P}{2} = \frac{w\ell}{2}$$

then,

$$M = \left(\frac{w\ell}{2}\right) \cdot \left(\frac{\ell}{x}\right) = \left(\frac{w \cdot \ell^2}{8}\right)$$

$$\Rightarrow x = 4$$

$$\therefore \text{Apply } \left(\frac{P}{2}\right) \text{ at } \left(\frac{\ell}{4}\right)$$

where:

- P = Applied Point Load (lb)
- w = Uniformly Distributed Load (lb/ft)
- ℓ = Span Length (ft)

The 6-inch steel tubes then transferred the load as line loads to the specimen. As not to jeopardize the strength of the furring assemblies, beneath the square tubes 0.50 inch thick strips of neoprene were placed between the furring strips. These neoprene pads held the square tubes up off the furring assemblies approximately 0.375 inch. The neoprene strips were 7 inches wide; spreading the load enough that it was determined compression of the ESP foam forms would not be enough to where the square tubes will come in contact with the furring assemblies. The illustration in Figure 12 shows the test set-up used in conducting the “HOBBS Wall” flexural strength test.



Figure 12. Full-Scale Test Set-Up

The load subjected to the wall specimen was measured using a single load cell at the location of the loading ram. The load cell was set up on steel plates in order to accommodate the stroke of the ram, and the ram pressed directly on the load cell. The following illustration shows the load loading ram and the load cell directly below.



Figure 13. Loading Ram and Load Cell

The vertical displacement of the specimens was measured at mid-width and quarter points along the length of the specimen. To ensure that the displacement readings are not altered by deformation of the EPS form; the draw-wire for the Displacement Transducer was attached directly to the concrete by means of a wooden block with an eyelet that was secured with a high strength epoxy. To get to the concrete on the underside of the wall specimens, the ESP foam form had to be removed; a 3-inch hole was made through the foam to the concrete “web” using a hole saw. The concrete was scraped clean to ensure a good bond of the epoxy. Directly below the cable, displacement transducers were placed and weighted down with steel plates to eliminate any movement during the testing. The following illustrations; Figure 14 and Figure 15, show the placement of the displacement transducers and shows the cables attached to the underside of the wall specimens.



Figure 14. Displacement Transducer Placement



Figure 15. Displacement Transducer Attached to the Specimen

The specimens were tested as simply-supported beams; therefore one end is pinned and the other is supported on rollers. The pinned-end will constrain any horizontal translation and vertical deflection, but will still allow rotation and not resist moment. An observation was made that the pinned connection was allowing some

slippage to occur; determined to be caused by the contact of the smooth steel on the slanted concrete surface not providing enough friction. To prevent this sliding, a sort of abutment was fabricated with points supporting the specimen end at the location of the neutral axis of the cross-section. The roller-end will constrain vertical deflection only, allowing horizontal translation and rotation to occur. This sort of abutment can be seen in the following illustration, Figure 16; notice the abutment is contacting the wall specimen at the location of the neutral axis of the section and the large steel plate is secured to the supporting double I-beam below.



Figure 16. Fabricated Abutment on Pinned-End

Early on there was an apparent concern that the testing apparatus might contact the PVC furring assembly at the supports. ‘Crushing’ of the furring assembly or the EPS foam was not to happen since this could jeopardize the strength of the wall specimens as well cause issues with the vertical displacement measurements. To circumvent such problems the specimens were to be supported in direct contact with the concrete “beams” at both the top and bottom of the specimen. The supports needed to be tall enough that there wasn’t going to be contact of the specimen to the support as it undergoes large

deflections during loading. The distance from the concrete surface, at the location of the beams, to the face of the furring assembly is 2.125 inch. A 3.5 inch steel pipe was chosen for the supports; this allowed enough clearance for large deflections. On the pinned-end of the specimen the steel pipe was welded to two 3 inch wide by 0.375 inch thick base plates that were then subsequently welded to the main large double I-beams on which the specimen supports are resting. The use of two base plates was to make up for the difference in concrete surface height due to the slanted bottom beam of the ICF wall system. On the roller-end of the specimen the base plate was placed between the steel pipe and the concrete surface as to prevent the possibility of local crushing of the concrete.

Behavioral Results

The two specimens that were tested behaved quite similar. Initial cracking of the concrete and EPS foam for the two specimens occurred at nearly identical loads and displacements; although beyond the cracking of the EPS foam the behavior of the specimens differed slightly. Wall Specimen #1 reached a maximum load value then dropped off slightly and stayed fairly constant at a lower load, approximately 90 percent of the maximum, up until complete failure. Wall Specimen #2 reached a maximum load and stayed rather constant up until complete failure. Wall #1 reached maximum capacity at a lower displacement and complete failure at a larger displacement than Wall #2; approximately 1.8 inches and 3.6 inches at the center of the wall, respectively. Wall #2 reached maximum capacity at approximately 2.0 inches of displacement at the center of the wall and 3.4 inches of displacement at the center of the wall for complete failure. These results can be seen in the following Figure 17.

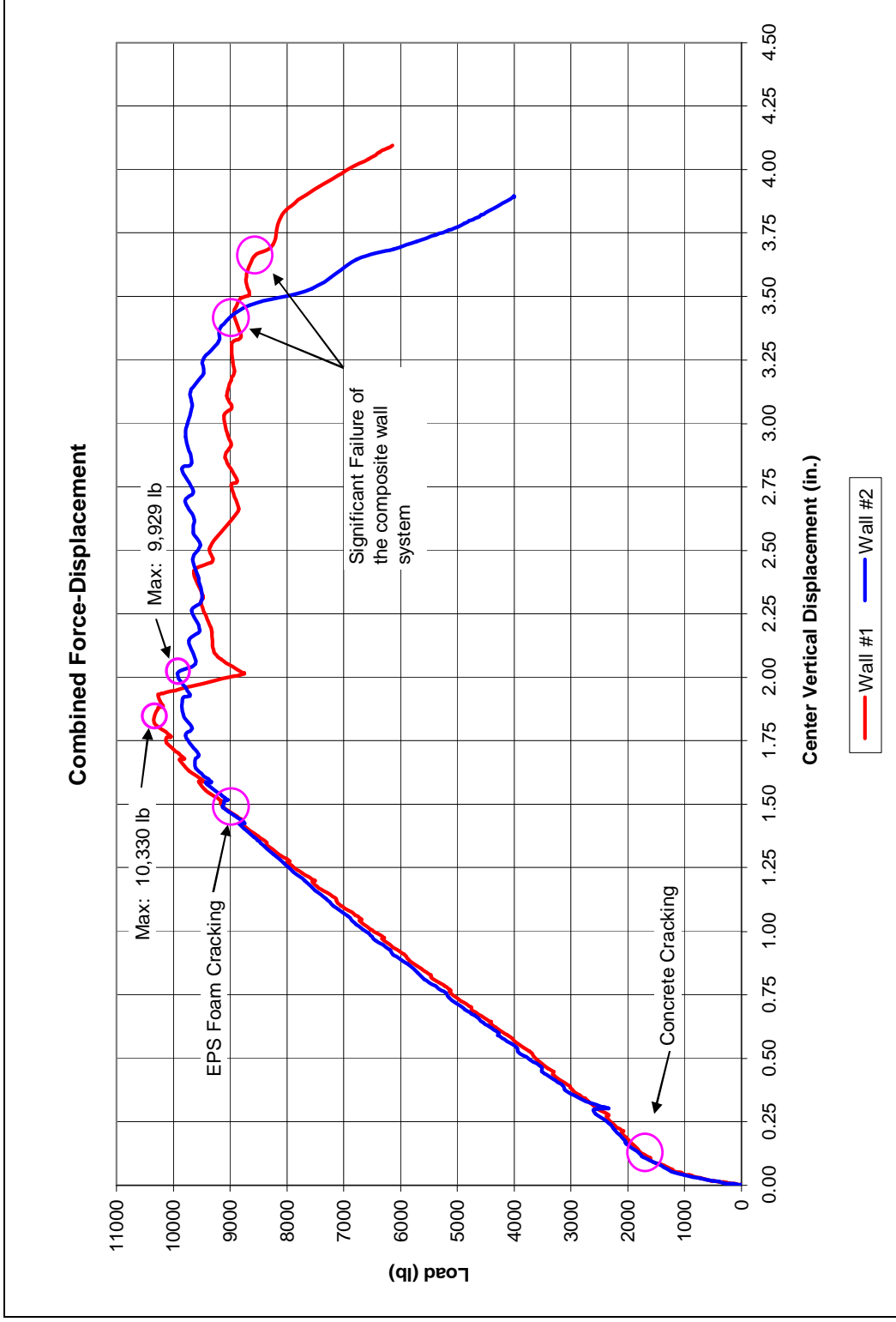


Figure 17. "HOBBS Wall" Force-Displacement

As was expected, initial cracking of the section occurred at the location of loading. This section is the most critical section since it is the location of maximum moment and high shear; these cracks are referred to as flexural-shear cracks and can be seen in the following illustration, Figure 18.

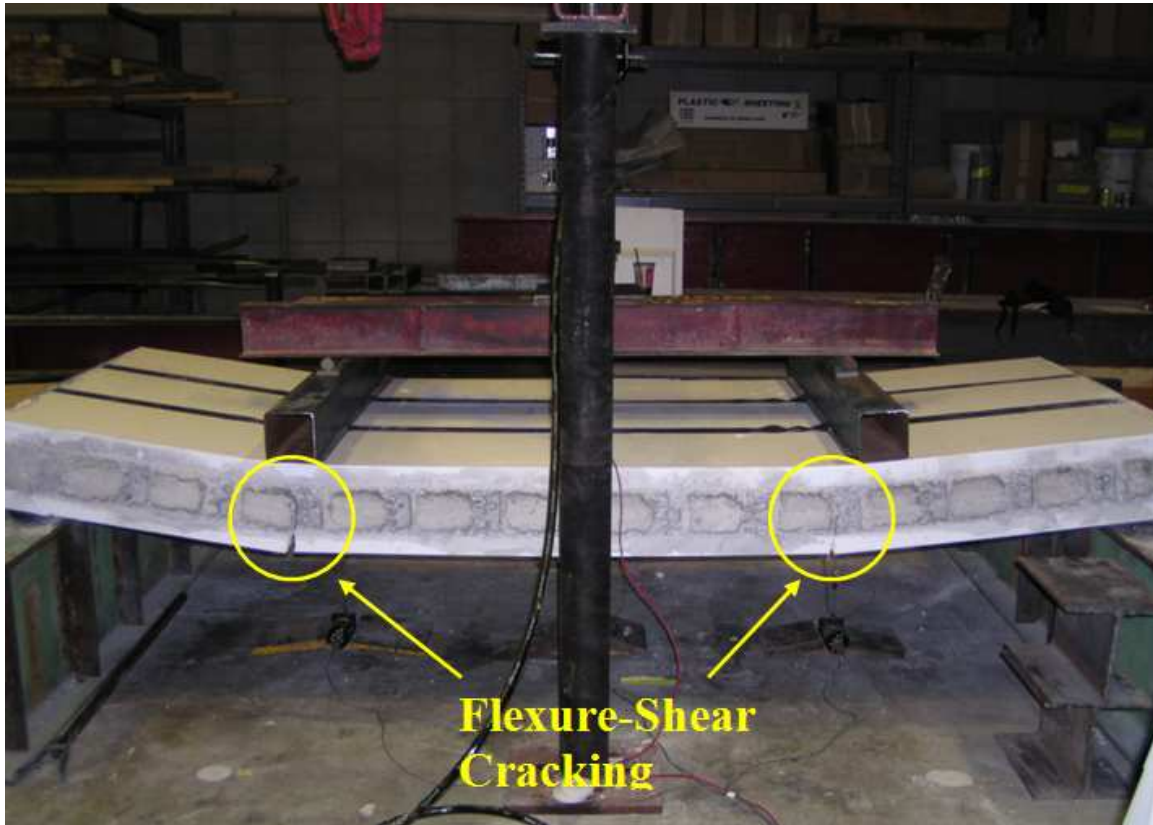


Figure 18. Flexural-Shear Cracking of the Specimen

As continued loading and deflection occurred it became quite visible that the furring assemblies were undergoing compression buckling on the upper side of the specimen, the top flange, and upon further inspection the observation was made that the bottom flanges of the furring assemblies of Specimen #2 experienced “necking” and fracture; this behavior indicates that the material had reached ultimate strength. These types of failures can be seen in the following illustrations of Figure 19 and Figure 20.

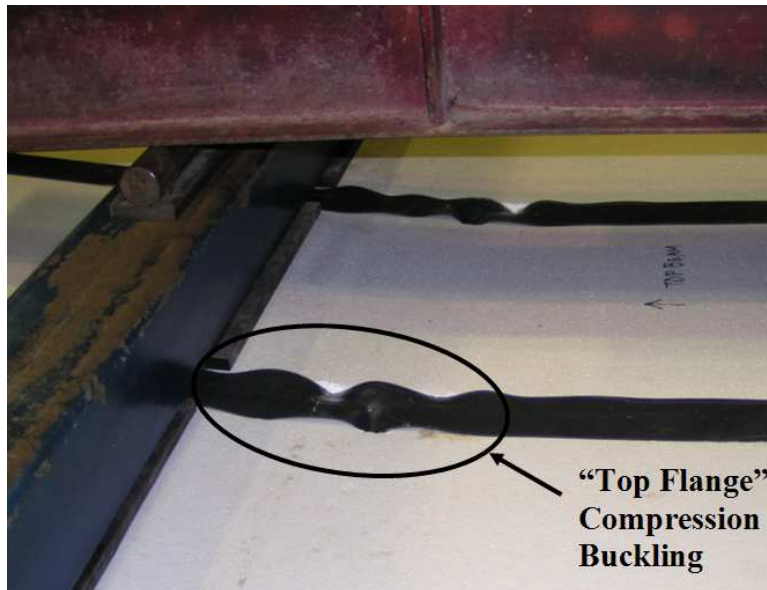


Figure 19. Compression Buckling on the Top Flange of the Furring Assembly



Figure 20. Furring Assembly Failure, "Necking" (left) and Fracture (right)

Observing such behaviors as seen in the preceding illustrations does not indicate there is significant slippage of the furring assembly within the wall section. In addition, the investigation of the specimen ends after the testing concluded did not show visible slippage of the furring assemblies.

ANALYSIS OF RESULTS

The data collected from the tests came as an electronic file for the wall flexural tests. The flexural strength data was analyzed using an Excel worksheet, as that was the most convenient with the number of data points obtained.

Full-Scale Wall Test

The key information obtained from the full-scale wall test was the flexural capacity due to a two-point line loading situation. The results were obtained as a single point load acting at the loading ram location. For the analysis an appropriate assumption was made that this load will exert equal forces at the two line load locations, also the self weight of the testing equipment will be presumed to be divided equally. The self weight of the concrete must also be taken into consideration when analyzing the applied load and capacity of the wall specimen.

Each full-scale wall specimen was determined to weigh 1383 lbs, based on a concrete unit weight of 150 lbs per cubic foot (pcf). This equates to an equivalent distributed load of 140.6 lbs per lineal foot (plf) of wall height. The total testing equipment weight resting on the wall specimen is 268 lb, or 134 lb each side. This load due to the testing equipment will give an initial moment induced on the wall specimen equal to 329.4 lb-ft, or 0.329 kip-ft at the mid length of the wall specimen due to the testing equipment and the concrete weight induces an additional moment of 1699.4 lb-ft, or 1.70 kip-ft at the mid length. Therefore, as the wall specimens sit unloaded there is an initial moment of approximately 2.03 kip-ft at mid-span.

Calculation 2. Determining Moment Induced by the Self Weight

$$Wt_{equip} = 268lb$$

then,

$$\frac{p}{2} = \frac{268lb}{2}$$

$$\Rightarrow \frac{P}{2} = 134lb$$

$$\gamma_{concrete} = 150 pcf \text{ (assumed)}$$

$$Wt_{concrete} = \left[\left(\frac{(3 \cdot (5.25in \cdot 4in + 12in \cdot 2in.))}{144in^2/ft^2} \right) \cdot (9.833 ft.) \right] \cdot 150 pcf$$

$$\Rightarrow Wt_{concrete} = 1383lb$$

$$w_{concrete} = \frac{1383lb}{9.833 ft}$$

$$\Rightarrow w_{concrete} = 140.6 lb./ft.$$

$$M_{selfwt.} = \left(\left(\frac{P}{2} \right) \cdot \left(\frac{\ell}{4} \right) \right) + \left(\frac{w \cdot \ell^2}{8} \right)$$

$$\Rightarrow M_{selfwt.} = \left((134lb) \cdot \left(\frac{9.833 ft.}{4} \right) \right) + \left(\frac{(140.6 lb./ft.) \cdot (9.833 ft.)^2}{8} \right)$$

$$\Rightarrow M_{selfwt.} = 2029.3^{lb-ft}$$

$$\Rightarrow M_{selfwt.} = 2.03^{k-ft}$$

where:

- Wt_{equip} = Total Testing Equipment Weight (lb)
- p = Applied Load (lb)
- $\gamma_{concrete}$ = Unit Weight of Concrete (pcf)
- $Wt_{concrete}$ = Total Weight of the Concrete (lb)
- $w_{concrete}$ = Equivalent Distributed Weight of the Concrete (lb/ft)
- $M_{selfwt.}$ = Moment Induced by the Self Weight (k-ft)

The first wall specimen reached a maximum applied load of 10,329.98 lb; 5,164.99 lb at each loading location. The second wall specimen reached a maximum

applied load of 9,929.09 lb; 4,964.55 lb at each loading location. The two tests give an average of 10,129.53 lb total load or 5,064.77 lb at each load point subjected to the wall.

Using the following simple calculation this equates to an equivalent distributed load:

Calculation 3. Equivalent Distributed Load

$$M = \left[\left(\frac{P}{2} \right) \cdot \left(\frac{L}{4} \right) \right] = \frac{w(L)^2}{8}$$

$$\Rightarrow \left[\left(\frac{10129.5lb}{2} \right) \cdot \left(\frac{118in./12in./ft.}{4} \right) \right] = \frac{w \left(\frac{118in./12in./ft.}{4} \right)^2}{8}$$

$$\Rightarrow w = 1030.12 plf$$

where:

- M = Moment (lb-ft)
- P = Total Applied Point Load (lb)
- L = Specimen Span Length (ft)
- w = Distributed Load (lb/ft)

Combining the applied load with the self weight of the wall and testing equipment, the first wall sustained a maximum nominal moment of 14.81 kip-ft and the second wall sustained 14.32 kip-ft, giving an average nominal moment capacity of 14.56 kip-ft for the 4 ft wall specimen. As is typical, the moment capacity can be thought of as moment capacity per foot of lineal wall length. For this particular test one can simply divide by the width of the wall, 4 feet; therefore, per foot of wall length the nominal moment capacity is equal to 3.64 kip-ft.

Conducting an analysis on the same steel-reinforced concrete wall section, but instead without the furring assemblies and EPS foam formwork in place; the moment at

which cracking occurs and the nominal moment capacity of the wall specimen are 2.026 kip-ft or 0.506 kip-ft per lineal foot of wall length and 9.76 kip-ft or 2.44 kip-ft per lineal foot of wall length, respectively. The cracking moment and applied moments equate to applied loads of 1648.3lb and 7940.3lb, respectively.

Calculation 4. Theoretical Cracking Moment

$$f_r = 7.5 \cdot \sqrt{f'_c}$$

$$\Rightarrow 7.5 \cdot \sqrt{2448 \text{ psi}}$$

$$\Rightarrow f_r = 371.1 \text{ psi}$$

$$I_g = \sum \left(\frac{b \cdot h^3}{12} \right)$$

$$\Rightarrow 3 \cdot \left[\left(\frac{4 \cdot (5.25)^3}{12} \right) + \left(\frac{12 \cdot (2)^3}{12} \right) \right]$$

$$\Rightarrow I_g = 168.7 \text{ in}^4$$

$$N.A. = \left(\frac{\sum A \cdot d}{\sum A} \right)$$

$$\Rightarrow \left[\frac{(2.625 \text{ in} \cdot ((3 \cdot 5.25 \text{ in} \cdot 4 \text{ in}) + (3 \cdot 12 \text{ in} \cdot 2 \text{ in})) + 3.75 \text{ in} \cdot (10.3 \cdot 0.62 \text{ in}^2))}{(3 \cdot 5.25 \text{ in} \cdot 4 \text{ in}) + (3 \cdot 12 \text{ in} \cdot 2 \text{ in}) + (10.3 \cdot 0.62 \text{ in}^2)} \right]$$

$$\Rightarrow N.A. = 2.675 \text{ in. (from extreme compression fiber)}$$

$$M_{cr} = \left(\frac{f_r \cdot I_g}{c} \right)$$

$$\Rightarrow \left(\frac{371.1 \text{ psi} \cdot 168.7 \text{ in}^4}{5.25 \text{ in} - 2.675 \text{ in}} \right)$$

$$\Rightarrow M_{cr} = 24312.5 \text{ lb-in}$$

$$\Rightarrow M_{cr} = 2.026 \text{ kip-ft}$$

where:

$f_r =$	Modulus of Rupture (psi)
$I_g =$	Gross Section Moment of Inertia (in ⁴)
$N.A. =$	Location of the Section Neutral Axis (in.)
$M_{cr} =$	Cracking Moment (k-ft)

Using the calculated cracking moment (M_{cr}), the load (P_{cr}) to induce this moment is determined.

Calculation 5. Theoretical Cracking Load

$$P_{cr} = \left(\frac{8 \cdot M_{cr}}{\ell} \right)$$
$$\Rightarrow \left(\frac{8 \cdot 2.026^{k-ft}}{\left(\frac{118in.}{12in./ft.} \right)} \right)$$
$$\Rightarrow P_{cr} = 1.648kip$$
$$\Rightarrow P_{cr} = 1648.3lb$$

where:

$$P_{cr} = \text{Cracking Load (lb)}$$

Notice that if the wall specimens were simple reinforced concrete, not incorporating the composite action of the EPS foam and PVC furring assemblies, the wall would nearly be cracking just setting up on the supports under the loading of the specimen's own self weight and testing equipment self weight.

Calculation 6. Theoretical Nominal Moment Strength

$$M_n = A_s \cdot f_y \cdot \left(d - \frac{a}{2}\right)$$

$$a = \frac{A_s \cdot f_y}{0.85 \cdot f_c' \cdot b}$$

$$\Rightarrow \frac{(0.62 \text{ in}^2 \cdot 63866.7 \text{ psi})}{(0.85 \cdot 2448 \text{ psi} \cdot 12 \text{ in.})}$$

$$\Rightarrow a = 1.586 \text{ in.} (\leq 1.625 \text{ in.})$$

then,

$$M_n = 0.62 \text{ in}^2 \cdot 63866.7 \text{ psi} \cdot \left(3.75 \text{ in.} - \frac{1.586 \text{ in.}}{2}\right)$$

$$\Rightarrow M_n = 117089 \text{ lb-in}$$

$$\Rightarrow M_n = 9.757 \text{ k-ft}$$

check strain,

$$c = \frac{a}{\beta_1}$$

$$\Rightarrow \frac{1.586 \text{ in}}{0.85}$$

$$\Rightarrow c = 1.866 \text{ in.}$$

$$\epsilon_s = \epsilon_{cu} \cdot \left(\frac{(d - c)}{c}\right)$$

$$\Rightarrow 0.003 \cdot \left(\frac{(3.75 \text{ in.} - 1.866 \text{ in.})}{1.866 \text{ in.}}\right)$$

$$\Rightarrow \epsilon_s = 0.00303 \text{ in./in.}$$

where:

M_n = Nominal Moment Capacity (k-ft)

a = Depth of the Compression Block (in.)

c = Depth of the Neutral Axis (in.)

ϵ_s = Steel Strain (in./in.)

ϵ_{cu} = Ultimate Allowable Concrete Compressive Strain (in./in.)

Using the calculated nominal moment (M_n), the load (P_n) to induce this moment is determined.

Calculation 7. Load Corresponding to Nominal Moment

$$P_n = \left(\frac{8 \cdot M_n}{\ell} \right)$$
$$\Rightarrow \left(\frac{8 \cdot 9.757^{k-ft}}{\frac{118in}{12in./ft.}} \right)$$
$$\Rightarrow P_n = 7.938kip$$
$$\Rightarrow P_n = 7937.9lb$$

where:

$$P_n = \text{Load Corresponding to Nominal Moment Capacity (lb)}$$

Observe that there is a difference of approximately 4.80 k-ft for the four foot wide specimen which equates to 1.20 k-ft difference in moment capacity per lineal foot of wall. In terms of distributed load this relates to approximately an additional 100 *plf* per foot of wall length. The large difference is believed to be a result of the composite action of the wall section, particularly the moment resistance provided by the PVC furring assemblies.

The displacement at mid-span of the full-scale wall specimens coinciding with each significant occurrence during loading can be observed on the force-displacement plot of Figure 17; 0.051 in. at the time the concrete cracked, 1.470 in. at the time the EPS foam cracked, and approximately 1.900 in. when the maximum flexural capacity was reached by yielding of the steel reinforcement. Comparing the experimental displacements to the theoretical displacements for the same steel-reinforced concrete wall section, but instead without the furring assemblies and EPS foam formwork in place

yields a maximum displacement at mid-span of 0.163 in. at which point the concrete will crack, and 2.891 in. when the maximum flexural capacity will be reached.

Calculation 8. Theoretical Displacement

$$E_c = 33 \cdot w^{(3/2)} \cdot \sqrt{f_c}$$

$$\Rightarrow 33 \cdot (144 \text{pcf})^{(3/2)} \cdot \sqrt{2448 \text{psi}}$$

$$\Rightarrow E_c = 2821391.7 \text{ psi}$$

$$n = \frac{E_s}{E_c}$$

$$\Rightarrow \frac{29000000 \text{psi}}{2821391.7 \text{psi}}$$

$$\Rightarrow n = 10.3$$

$$\frac{b \cdot (kd)^2}{2} - n \cdot A_s \cdot (d - kd) = 0$$

$$\Rightarrow \frac{12 \text{in.} \cdot (kd)^2}{2} - 10.3 \cdot (0.62 \text{in}^2) \cdot (3.75 \text{in.} - kd) = 0$$

$$\Rightarrow kd = 1.535 \text{in.}$$

$$I_{cr} = I_{concrete} + I_{steel}$$

$$I_{concrete} = \frac{1}{3} \cdot (b) \cdot (kd)^3$$

$$\Rightarrow \frac{1}{3} \cdot (12 \text{in.}) \cdot (1.535 \text{in.})^3$$

$$\Rightarrow I_{concrete} = 14.476 \text{in}^4$$

$$I_{steel} = n \cdot (A_s) \cdot (d - kd)^2$$

$$\Rightarrow 10.3 \cdot (0.62 \text{in}^2) \cdot ((3.75 - 1.535) \text{in.})^2$$

$$\Rightarrow I_{steel} = 31.331 \text{in}^4$$

then,

$$I_{cr} = 14.476 \text{in}^4 + 31.331 \text{in}^4$$

$$\Rightarrow I_{cr} = 45.807 \text{in}^4$$

$$\begin{aligned} \Delta &= \left(\frac{P}{24E_c I} \right) \cdot \left(\frac{\ell}{4} \right) \cdot \left(3\ell^2 - 4 \cdot \left(\frac{\ell}{4} \right)^2 \right) \\ \rightarrow \Delta_{cr} &= \left(\frac{P_{cr}}{24E_c I_g} \right) \cdot \left(\frac{\ell}{4} \right) \cdot \left(3\ell^2 - 4 \cdot \left(\frac{\ell}{4} \right)^2 \right) \\ \Rightarrow &\left(\frac{1648.3lb}{24 \cdot (2821391.7 \text{ psi}) \cdot (168.7in^4)} \right) \cdot \left(\frac{118in.}{4} \right) \cdot \left(3(118in.)^2 - 4 \cdot \left(\frac{118in.}{4} \right)^2 \right) \\ \Rightarrow \Delta_{cr} &= 0.163in. \\ \rightarrow \Delta_n &= \left(\frac{P_n}{24E_c I_{cr}} \right) \cdot \left(\frac{\ell}{4} \right) \cdot \left(3\ell^2 - 4 \cdot \left(\frac{\ell}{4} \right)^2 \right) \\ \Rightarrow &\left(\frac{7937.9lb}{24 \cdot (2821391.7 \text{ psi}) \cdot (45.807in^4)} \right) \cdot \left(\frac{118in.}{4} \right) \cdot \left(3(118in.)^2 - 4 \cdot \left(\frac{118in.}{4} \right)^2 \right) \\ \Rightarrow \Delta_n &= 2.892in. \end{aligned}$$

where:

- E_c = Modulus of Elasticity of Concrete (psi)
- n = Factor for Transformed Section
- kd = Depth of Cracked Section Compression Block (in.)
- I_{cr} = Cracked Section Moment of Inertia (in⁴)
- Δ = Deflection (in.)

The theoretical displacement at which cracking will occur and when the section will reach maximum capacity are both higher than what was experienced experimentally in the full-scale testing.

The following, Figure 21, shows an idealized force-deflection comparison of full-scale wall specimen results to a theoretical wall consistent with that of the “HOBBS Wall” section, but without the EPS foam and PVC furring assembly influence. An idealized moment vs. displacement comparison can be seen in the Appendix.

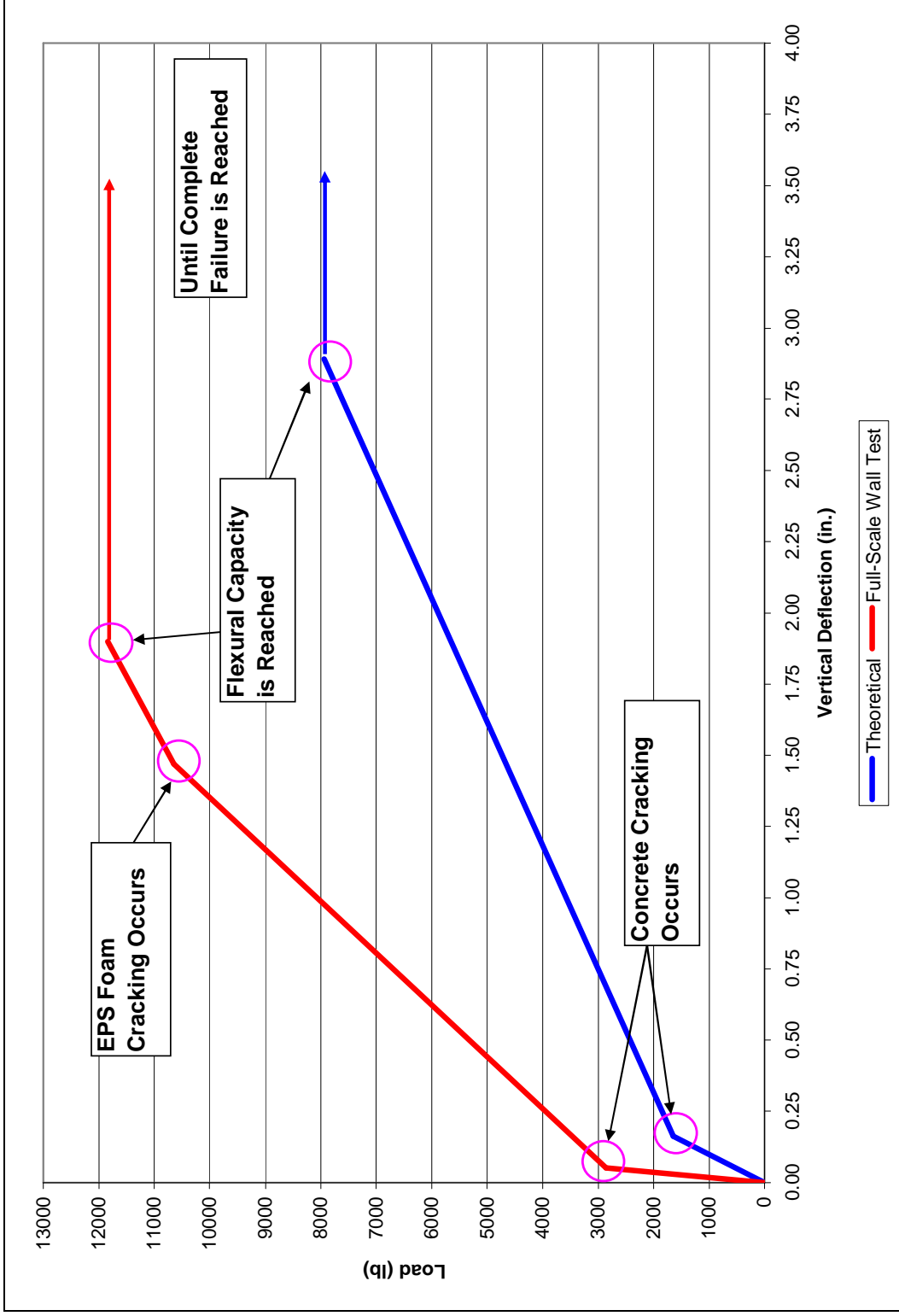


Figure 21. Idealized Force-Displacement Comparison

For additional comparison the capacity of a wall with uniform thickness equal to that of the columns and beams in the “HOBBS Wall” system, 5.25 inches, was analyzed. The section was taken as steel-reinforced concrete, again without any furring assembly or EPS foam introduced. The nominal moment capacity was determined to be 11.72 kip-ft for a four foot wall length like that of the test specimens, or equivalently, 2.93 kip-ft per foot of lineal wall length.

Considering the applied load and the self weight of the wall specimens and testing equipment it was determined that the first wall sustained a shear force of 6.025 kips; and the second wall a shear force of 5.825 kips, this yields an average of 5.925 kips for the 4 foot wall specimen. Therefore, the average shear induced, at maximum flexural capacity, per unit length of wall is 1.481 kips. With the four-point scheme that was used for testing, this maximum shear force is constant from both supports up to the location of applied load. And between the loading points the shear, in theory, is equal to zero.

SUMMARY AND CONCLUSIONS

The conducted tests offered insight into the flexural strength capacity of the “HOBBS Wall” system. The flexural strength capacity of the system was determined based on the average of two specimens tested.

The flexural tests yielded an average nominal moment capacity of 12.451 k-ft or 3.113 k-ft per lineal foot of wall length due to applied loads and a total of 14.56 kip-ft or 3.64 kip-ft per lineal foot of wall length including the contribution of the self weights of the testing equipment and wall specimen. The flexural tests induced an average shear force of 5.925 k or 1.481 k per lineal foot of wall length at maximum flexural capacity.

Upon the completion of the tests the wall specimens were investigated and the observation was made that the EPS foam remained well bonded to the concrete core. This finding was positive, signifying that the section was acting as a composite section. The unbroken bond will increase the flexural strength capacity of the ICF wall section. The furring assemblies underwent considerable compression buckling at the top flange and in some cases “necking” and fracture at the bottom flange; seeing these behaviors of the furring assemblies does not indicate there is significant slippage of the furring assembly within the wall section and that the wall section is likely gaining strength from this composite action. Hence, the composite wall section of the “HOBBS Wall” was determined to provide additional capacity, approximately 4.80 k-ft for the four foot wide specimen, when compared to that of a comparable reinforced concrete section not incorporating the EPS foam or PVC furring assemblies. Therefore, one could attribute the additional moment capacity of the “HOBBS Wall” system to be a contribution of the moment couple developed by the PVC furring assemblies and EPS foam formwork.

ACKNOWLEDGEMENTS

The preceding research and testing was conducted at the Iowa State University Structural Engineering Laboratories in Department of Civil, Construction, and Environmental Engineering. The testing and analysis was funded through the Technical Assistance Program through the Institute for Physical Research and Technology (IPRT) in conjunction HOBBS Building System LLC who provided the materials and labor to construct the walls. Acknowledgement must go to Andrew Hobbs and the HOBBS Building System crew for their time and effort throughout the project. Andrew's advice, feedback, and patience were very much appreciated. Acknowledgement must also go to Lynne Mumm, Technology Commercialization Program Manager of IPRT Company Assistance, who arranged the budgeting of the project.

The authors would like to especially acknowledge Douglas L. Wood, the Structural Engineering Laboratory Supervisor. His knowledge and assistance throughout the entire project were very useful and without his help, this project would not have been possible. Thanks go to the undergraduate students who provided their time and efforts in the construction and casting of the walls, casting of concrete cylinder specimens, and the setup of the full-scale wall testing frame.

REFERENCES:

1. Panushev, I. S., VanderWerf, P.A., Insulating Concrete Forms Construction, McGraw-Hill Companies, New York, 2004.
2. VanderWerf, P.A., Feige, S. J., Chammas, P., Lemay, L. A., Insulating Concrete Forms, McGraw-Hill Companies, New York, 1997.
3. Porter, M. L., Dreyer, D. R., Elemental Beam and Shear Testing of GFRP Sandwich Wall Connectors, Iowa State University, Ames, Iowa, CATD Project 97-19, 1997.
4. Van Geem, M. G., Shirley, S. T., Heat Transfer Characteristics of Insulated Concrete Sandwich Panel Walls, Composite Technologies Corporation, Construction Technology Laboratories, Illinois, 1986.
5. Department of Energy. Insulation Fact Sheet – R-Value Recommendations for New Buildings. January 2008.
< http://www.ornl.gov/cgi-bin/cgiwrap?user=roofs&script=ZipTable/ins_fact.pl >
6. Porter, M. L., Post, A. W., Thermal and Fatigue Testing of Fiber Reinforced Polymer Tie Connectors Used in Concrete Sandwich Walls, Iowa State University, Ames, Iowa, 2006.

7. Building Code Requirements for Structural Concrete (ACI 318-08) and Commentary, American Concrete Institute, Farmington Hills, Michigan, 2008.

Appendix: Additional Plots and Figures

